Review Article

Innovative treatment for hepatocellular carcinoma (HCC)

Junichi Kaneko[1,2], Takashi Kokudo[1,2], Yoshinori Inagaki[1,2], Kiyoshi Hasegawa[1,2]

[1]Division of Hepato-Biliary-Pancreatic Surgery, [2]Division of Artificial Organ and Transplantation, Department of Surgery, Graduate School of Medicine, The University of Tokyo, Bunkyo-ku, Tokyo, Japan

Contributions: (I) Conception and design: K Hasegawa; (II) Administrative support: K Hasegawa; (III) provision of study materials or patients: J Kaneko, T Kokudo, Y Inagaki; (IV) Collection and assembly of data: J Kaneko, T Kokudo, Y Inagaki; (V) Data analysis and interpretation: J Kaneko, T Kokudo, Y Inagaki; (VI) Manuscript writing: All authors; (VII) Final approval of manuscript: All authors.

Correspondence to: Kiyoshi Hasegawa. The University of Tokyo, 7-3-1 Hongo, Bunkyo-ku, Tokyo 113-8655, Japan. Email: hasegawa-2su@h.u-tokyo.ac.jp.

Abstract: Indocyanine green (ICG) is not new in the field of liver surgery. Early studies performed in the 1980s and 1990s revealed the value of the ICG clearance test in predicting post-hepatectomy morbidity and mortality. ICG clearance and retention tests are crucial for determining precise liver function before liver surgery and offer several benefits for safe surgery. Whereas ICG is well-known and has long history in medicine, recent progress in infrared light technology over the last decade has highlighted another feature of ICG. For example, ICG fluorescence-guided surgery may change the next generation of liver surgery. In the near future, ICG with near-infrared (NIR) light photodynamic therapy (PDT) is expected to become a new treatment method for hepatocellular carcinoma (HCC). Furthermore, several aspects of the mechanisms of ICG accumulation in HCC cells have been revealed by important basic research studies. New imaging technologies and mechanistic findings keep ICG in the spotlight. In this article, we review three recently described topics of ICG which may contribute to the development of innovative and new treatments method for HCC, fluorescence-guided surgery, mechanism of ICG accumulation in HCC cells, PDT for HCC.

Keywords: Indocyanine green (ICG); fluorescence-guided surgery; accumulation mechanism; photodynamic therapy (PDT); near-infrared light (NIR light)

Received: 03 July 2018; Accepted: 15 October 2018; Published: 22 October 2018.
doi: 10.21037/tgh.2018.10.04
View this article at: http://dx.doi.org/10.21037/tgh.2018.10.04

Introduction

Indocyanine green (ICG) is not new in the field of liver surgery. Early studies performed in the 1980s and 1990s revealed the value of the ICG clearance test in predicting post-hepatectomy morbidity and mortality (1,2). ICG clearance and retention tests are crucial for determining precise liver function before liver surgery and offer several benefits for safe surgery (3). Recent progress in infrared light technology over the last decade has highlighted another feature of ICG. In this article, we review three recently described features of ICG that may contribute to the development of innovative treatments for hepatocellular carcinoma (HCC).

Fluorescence-guided surgery for HCC

Anatomical resection

Liver resection is the first-line curative treatment for HCC (4). Anatomical liver resection was first reported by Makuuchi *et al.* in 1985 (5), who injected indigo-carmine into a branch of the portal vein. Several studies since then have demonstrated a survival benefit of anatomical liver resection compared to non-anatomical liver resection (6,7). Accurate Anatomical resection requires identification of the liver segments before parenchymal transection (8). Beside injection of indigo-carmine, segment boundaries can be identified by isolating and clamping the corresponding

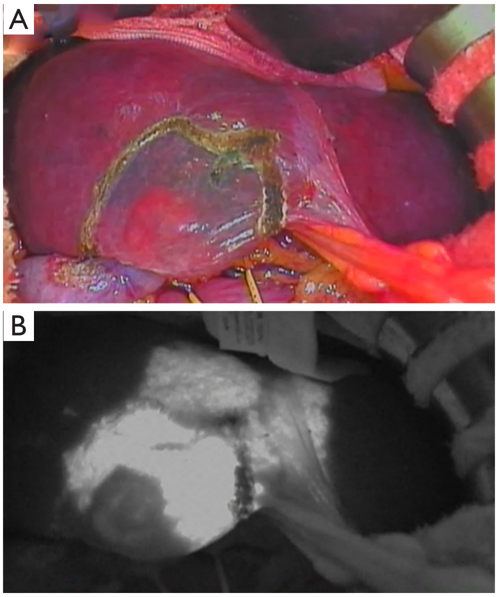

Figure 1 Identification of liver segment boundaries by injecting indocyanine green into the inferior branch of the portal vein for Couinaud's segment IV. (A) Without fluorescence imaging; (B) under fluorescence imaging.

Glissonian sheaths (9,10). These techniques, however, do not always provide clear identification of the segment boundaries, especially in patients with cirrhosis and/or undergoing repeated hepatectomy (11,12).

To overcome the limitations of these methods, ICG injection into the corresponding branch of the portal vein was proposed (8,13). As initially reported by Aoki *et al.* (13,14), portal vein branches feeding the HCC-bearing hepatic segment are punctured under intraoperative ultrasonography and fluorescence images of the liver surfaces are obtained using an infrared camera and amplifier (*Figure 1*). Aoki *et al.* showed that the ICG staining technique identified stained subsegments and segments in 90% (73/81) of patients. They also reported that the detection rate of the liver segment boundaries did not differ significantly between non-cirrhotic liver and cirrhotic liver (9). Miyata *et al.* reported that identifying hepatic segments using ICG fluorescence imaging enhances the accuracy of anatomical segmentectomy compared with the conventional technique using indigo-carmine (8). In their study, the ICG staining technique was effective in all 30 patients (100%), whereas the indigo-carmine technique was effective in only 17 patients (57%). The ICG staining technique was especially effective in cases that underwent repeated liver resection for HCC recurrence (8). In cases in which multiple branches of the portal vein feed the HCC-bearing hepatic segment, multiple staining and counterstaining using ICG can also be performed, similar to conventional indigo-carmine staining (11,15). Fusion ICG fluorescence imaging, which provides both fluorescence images and macroscopic views on a single screen, may be more effective for obtaining a clear demarcation line to enhance the accuracy of parenchymal dissection (16). The feasibility and clinical utility of projection mapping with ICG fluorescence to identify anatomical landmarks for parenchymal dissection were recently reported (17).

Laparoscopic liver resection for HCC has developed rapidly and is considered a standard treatment strategy, especially for minor liver resection (18). Furthermore, in specialized centers for laparoscopic liver surgery, laparoscopic anatomical liver resection is also performed (19). Ishizawa *et al.* initially reported application of the ICG staining technique for laparoscopic anatomical resection (20). Recently, Ueno *et al.* reported a combination of an interventional radiology technique with laparoscopic liver segmentation (21). A catheter is inserted from the femoral artery into the targeted arterial branch feeding the segment in a hybrid operating room. After confirming the perfusion area by arteriography, an embolic solution containing ICG is injected and the demarcation line identified by ICG fluorescence imaging. Because the conventional puncture technique may sometimes be difficult in a laparoscopic setting due to limited access, this new procedure may be a good alternative in laparoscopic surgery for identifying the demarcation lines of liver segments.

Inflow and outflow evaluation

Inflow and outflow evaluation of the liver is also important for performing safe liver surgery, especially in living-donor liver transplantation (22,23). After reconstruction of the hepatic vessels, ICG administration allows for clear visualization of the reconstructed hepatic artery and portal vein on the fluorescence images (24,25). Kawaguchi *et al.* reported that veno-occlusive regions and non-veno-occlusive regions can be visualized after intravenous injection of ICG, with ICG concentrations significantly lower in the veno-occlusive regions than in the non-veno-occlusive regions (26). These findings indicate that intraoperative ICG-fluorescence imaging enables real-time visualization of non-veno-occlusive, veno-occlusive, and ischemic regions, and evaluation of the extent of the functional outflow decrease.

Cholangiography

Cholangiography is performed for intraoperative visualization of the biliary tract to avoid injury of the bile duct (27). Routine cholangiography is recommended during cholecystectomy and is an essential procedure during donor hepatectomy to divide the bile duct at the appropriate level (28,29). Conventional radiographic cholangiography has several drawbacks, however, including exposure of the medical staff to radiation, and the need for a large C-arm fluoroscopic machine and trans-cystic tube for injecting the contrast medium. Ishizawa *et al.* reported intraoperative fluorescence cholangiography by intravenous injection of ICG (30). In their study, the common hepatic duct was identified in all 10 patients after intravenous ICG injection, similar to the results of intrabiliary injection of ICG in 13 patients. Schols *et al.* reported that ICG was visible in the bile duct within 20 minutes after injection and remained there for up to approximately 2 h in 30 patients undergoing laparoscopic cholecystectomy (31,32). The common bile duct was identified in 83% of the cases and the cystic duct was identified in 97% of the cases using ICG cholangiography. The usefulness of ICG cholangiography has also been reported in donor hepatectomy and laparoscopic hepatectomy (33,34).

In addition to visualizing the biliary tracts, ICG is useful for real-time detection of bile leaks during hepatectomy (35,36). Kaibori *et al.* reported a randomized controlled trial enrolling 102 patients who underwent hepatic resection without biliary reconstruction. The patients were randomly divided in two groups with or without ICG fluorescence cholangiography and sites of bile leakage were closed by suture or ligation. Five patients developed postoperative bile leakage in the control group compared with no bile leakage in the ICG cholangiography group (10% *vs.* 0%, P=0.019). Thus, ICG cholangiography may be useful for preventing bile leakage after hepatic resection.

Tumor visualization

Identification of small HCCs is important for curative resection and improvement of patient outcomes. In addition, clear delineation between tumor and normal tissue is important to obtain safe surgical margins. In 2009, real-time identification of HCC using ICG fluorescence imaging was reported (37,38). This technique is based on the ICG accumulation characteristics of HCC. Gotoh *et al.* reported the ICG fluorescence technique in 10 patients with solitary HCC who underwent hepatectomy (37). ICG was injected intravenously several days before surgery. All the HCCs were detected by ICG fluorescence and completely removed with negative margins using the fluorescence images as a guide. In four cases, new HCC nodules were detected by ICG fluorescence. Ishizawa *et al.* reported the results of 20 HCC patients who underwent ICG fluorescence imaging of the liver surfaces before hepatic resection (38). ICG fluorescence imaging before resection identified 21 of 41 HCCs (51%). Tumors that were not identified by intraoperative ICG fluorescence imaging were smaller than the identifiable tumors and the tumor location was deeper. None of the tumors located deeper than 8 mm from the liver surface were detected. In the surgical specimens, ICG fluorescence imaging identified all HCCs. Well-differentiated HCCs appeared as uniformly fluorescing lesions with a higher lesion-to-liver contrast than poorly differentiated HCCs (39). Fluorescence microscopy revealed an accumulation of ICG in the cytoplasm of HCC cells (38). This ICG fluorescence imaging system can also be applied for intraoperative detection of extrahepatic metastasis in HCC patients (40).

The accuracy of intraoperative diagnosis in laparoscopic liver resection might be inferior to that in open surgery because the ability to visualize and palpate the liver surface during laparoscopy is relatively limited. Kudo *et al.* reported the results of ICG-fluorescence imaging in 10 HCC patients who underwent laparoscopic hepatectomy (41). Similar to the open technique, ICG was administered intravenously within the 2 weeks prior to surgery (38). ICG fluorescence images of the liver surfaces were obtained intraoperatively during mobilization of the liver using a laparoscopic fluorescence imaging system. In 16 resected HCCs, laparoscopic ICG fluorescence imaging identified 12 HCCs (75%) on the liver surfaces distributed over all Couinaud's segments, including tumors that had not been identified in normal color images. Similar to the results of open ICG fluorescence imaging, tumors that were identified by fluorescence imaging were located closer to the liver surface than tumors that were not identified by fluorescence imaging (38,41). Like palpation during open hepatectomy, laparoscopic ICG fluorescence imaging enables real-time identification of subcapsular liver cancers (*Figure 2*). Terasawa *et al.* reported fusion-fluorescence imaging using ICG in laparoscopic hepatectomy (42). This technique provides real-time identification of the tumor and may facilitate estimation of the required extent of hepatic mobilization and determination of the appropriate liver transection line.

Figure 2 Identification of hepatocellular carcinoma using indocyanine green fluorescence imaging (PINPOINT, Stryker Japan K.K., Tokyo, Japan).

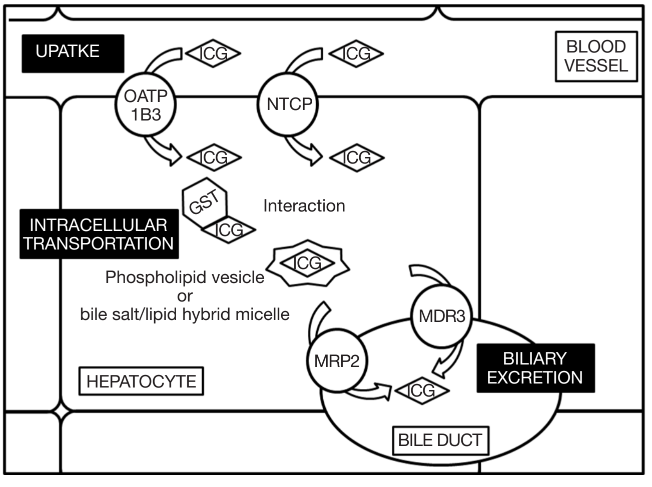

Figure 3 The suggested mechanism of hepatic metabolism of ICG. Hepatic uptake of ICG is facilitated by OATP1B3 and NTCP. During the intracellular transportation of ICG, it binds to the GST isozyme, forming phospholipid vesicles and bile salt/lipid hybrid micelles. Biliary excretion is facilitated by MDR3 and MRP2. ICG, indocyanine green; NTCP, Na^+-taurocholate co-transporting polypeptide; GST, glutathione S-transferase.

New fluorescence agents for liver surgery

Since the approval of ICG by the US Food and Drug Administration, it has been widely used for liver function analysis in HCC patients with well-established safety, and fluorescence imaging techniques for HCC mainly use ICG (43). Several other agents have been proposed for fluorescence imaging in liver surgery, but their clinical use and evidence are limited. The porphyrin precursor 5-aminolevulinic acid, approved as a fluorescence imaging agent in the clinical setting, is useful for intraoperative detection of liver tumors and bile leakage (44,45). Kaibori *et al.* reported that fluorescence imaging using 5-aminolevulinic acid may provide better specificity for detecting surface-invisible malignant liver tumors than ICG fluorescence imaging alone (44). In a porcine model, Matsui *et al.* reported the usefulness of methylene blue for visualizing extrahepatic bile ducts during cholecystectomy (46). In a rat model, sodium fluorescein, which can be visualized without a specific fluorescence-detecting camera when exposed to blue light, is useful for visualizing hepatobiliary structures (47).

In addition to the already approved fluorescence agents, new agents have also been reported in a preclinical setting. Zeng *et al.* synthesized arginine-glycine-aspartic acid-conjugated highly loaded ICG mesoporous silica nanoparticles as a fluorescent probe and explored its application to intraoperative imaging of liver tumors (48). In a mouse model, the probe accurately delineated tumor margins and detected microtumors (<2 mm) that could not be detected by ICG fluorescence imaging. Andreou *et al.* synthesized silica-encapsulated surface-enhanced Raman scattering nanoparticles that act as a molecular imaging agent for liver tumors (49). This imaging system delineated tumors more accurately and was less susceptible to photobleaching than fluorescence imaging using ICG in a mouse model. Although the findings require clinical confirmation, these new materials could be promising fluorescence agents to improve the accuracy of fluorescence imaging in liver surgery.

Mechanism of ICG accumulation in HCC cells

Hepatocyte metabolism is complex. Various transporter proteins are involved in hepatic clearance of compounds. The accumulation of ICG, an anionic compound, is thought to be induced by altering those transporters as well as the morphologic changes to HCC tissues due to cancer progression. The biologic mechanism of uptake, intracellular transportation, and biliary excretion of ICG in hepatocytes are suggested as shown in *Figure 3*, but the exact pathway of hepatic metabolism of ICG remains to be elucidated.

Hepatic uptake of anionic compounds is accomplished by organic anion transporting polypeptides (OATP), organic anion transporters (OAT), and Na^+-taurocholate co-transporting polypeptide (NTCP) (50-52). Biochemical studies revealed that ICG inhibits the activity of OATP1B1, OATP1B3, OATP2B1, and NTCP in a dose-dependent manner (53,54). Therefore, those transporter proteins are suggested to interact with ICG. Genetic analysis was performed to elucidate the transporters that take-up ICG into the hepatocytes. Cell biology studies using Chinese hamster ovary cells showed that ICG uptake is enhanced in OATP1B3-transfected cells and NTCP-transfected cells compared with wild-type cells (54). These findings suggested that OATP1B3 and NTCP mainly contribute to ICG uptake in hepatocytes. Subclinical studies also demonstrated a relationship between the expression of those transporters and ICG clearance. A case report of an HCC patient with an ICG excretory defect showed that OATP1B3 was downregulated in both the cancerous and non-cancerous tissues (55). In this case, however, the expression of other transporters, including NTCP, was not downregulated. Patients with Rotor syndrome presenting with conjugating hyperbilirubinemia are also negative for OATP1B3 expression (56). The cause of the OATP1B3 downregulation in these patients is suggested to be a homozygous insertion of long-interspersed element-1 in intron 5 of the *Slco1b3* gene as well as a homozygous mutation of the *Slco1b1* gene (56). As described above, OATP1B1 is not a main contributor to ICG uptake in hepatocytes. Therefore, genetic alteration of the *Slco1b3* gene is suggested to induce the ICG excretory defect via OATP1B3 downregulation. Another genetic study using tissues of patients with liver diseases also revealed that all patients were positive for long-interspersed element-1 insertion in intron 5 of the *Slco1B3* gene and negative for OATP1B3 protein expression (57). These results indicated that alterations of OATP1B3 expression significantly affect the hepatic clearance of ICG in patients with liver disease, suggesting that the accumulation of ICG in HCC tissues is induced by OATP1B3 overexpression. Gene set enrichment analysis revealed upregulation of *Slco1B3* and *NTCP* in cancerous tissue compared with non-cancerous tissue in HCC patients with ICG accumulation (58). The protein expression of OATP1B3 and NTCP was higher in the HCC tissues of patients showing cancerous-type ICG fluorescence compared with those showing rim-type ICG fluorescence (58). On the basis of these biologic and subclinical studies, the accumulation of ICG in HCC tissues is suggested to be induced by enhanced ICG uptake via the overexpression of OATP1B3 and NTCP.

On the other hand, alterations of the ICG excretion system have also been examined. ICG is a hydrophobic organic anion excreted in bile (59), and it is associated with phospholipid vesicles and bile salt/lipid hybrid micelles (60). Microscopic analysis shows higher ICG fluorescence in the perinuclear granule/vesicles of wild-type Chinese hamster ovary cells (54). Series of transporters including the multidrug resistance (*Mdr*) genes and multidrug resistance-associated protein (*Mrp*) genes mediate biliary excretion of various substances. Huang *et al.* studied the role of *Mdr2* in ICG excretion using their established *Mdr2*$^{-/-}$ mice and clarified that the biliary excretion of ICG in *Mdr2*$^{-/-}$ mice is significantly decreased by 90% compared with the wild-type (61). Immunoblot analysis of the expression of MDR3, the human homologous gene of *Mdr2*, in HCC tissues indicated that MDR3 expression is significantly higher in HCC tissues with ICG accumulation than in those without ICG accumulation (62). In immunohistochemical analysis, however, the expression of MDR3 was not significantly related with ICG accumulation in HCC tissues (62). According to the results of these studies, alterations in MDR3 expression do not always induce ICG accumulation. The gene set enrichment analysis performed by Ishizawa *et al.* also indicated MRP2 upregulation in cancerous tissue compared with non-cancerous tissue in HCC patients with ICG accumulation (58). MRP2 is a canalicular multispecific OAT and functions to excrete various substrates into the bile (63). Thus, MRP2 was considered to contribute to the bile excretion of ICG. In a study using Mrp2-deficient rats, however, bile excretion of ICG decreased only 25% to 75% in those rats compared with the wild-type, and the cause of this partial decrease was suggested to be alterations of intracellular transportation properties of ICG and not decreased transportation across the hepatocyte canalicular membrane (64-66). ICG is suggested to bind some glutathione S-transferase (GST) isozymes, which contributes to the intracellular transportation of organic anions (66). A biochemical study using mutant rats with hyperbilirubinemia indicated that the decreased binding of ICG to cytosolic proteins, e.g., GSTs, may impair the biliary excretion of ICG (66). The gene set enrichment analysis performed by Ishizawa *et al.*, however, indicated the upregulation of GST theta-1 (GSTT1) in cancerous tissue compared with non-cancerous tissue in HCC patients with ICG accumulation (58). On the basis of this result, expression of the target cytosolic protein that interacts with ICG is not considered to decrease in HCC cells. Further studies are necessary to clarify the mechanism of intracellular transportation of ICG, which has an important relation to the biliary excretion of that compound. Although

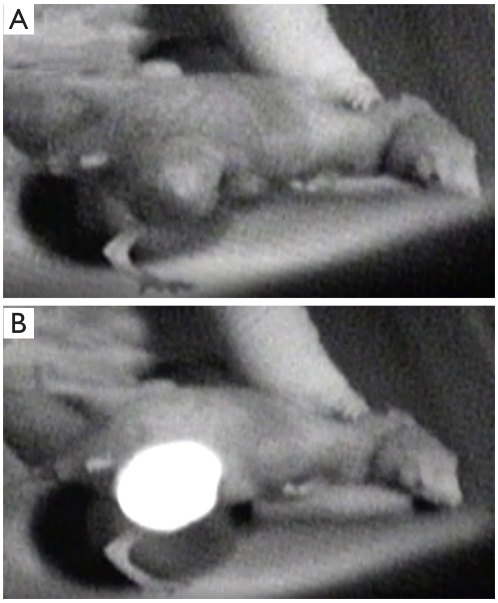

Figure 4 HuH-7 xenograft tumors were observed in the center of abdomen of the transplanted mice (A). Twenty-four hours after ICG administration, HuH-7 xenograft tumors in mice exhibited uniform fluorescence under the fluorescence imaging system (B). ICG, indocyanine green.

multiple pathways for the transport of organic anions across the canalicular membrane were clarified, the mechanism of biliary excretion of those anions with high hydrophobicity such as ICG remains controversial.

Photodynamic therapy (PDT) for HCC

PDT is a noninvasive treatment that combines a photosensitizer and an activating light source. Although it is effective for only a limited area, PDT is a well-established clinical treatment for various cancers developing in limited and superficial tissues, such as skin cancer (67), Barrett's esophagus and/or esophageal cancer (68), bladder cancer (69), and early-stage lung cancer (70). There are, however, two important obstacles. One is that the photosensitizer has weak tumor selectivity, and the other is the shallow light penetration ability. Consequently, PDT is not optimal for treating solid tumors or cancers.

Although the prognosis of patients with HCC has remarkably improved over the last 50 years, new treatment methods using next generation medicine are eagerly anticipated. ICG fluorescence in HCC was discovered in 2009 (38), and researchers have fervently evaluated this phenomenon. Because ICG has high HCC specificity, it is a photosensitizer and absorbs near-infrared (NIR) light. Although these features lead to the hypothesis that PDT may become a reality for HCC, reports supporting this hypothesis are still scarce.

NIR light has some advantages. The penetration depth of NIR light ranges from 7 to 10 mm (71,72), up to several centimeters, which is deeper than any other light sauce. In a clinical setting, dermatologists use PDT in combination with ICG and NIR light to treat port-wine stains (73). There are no reports, however, of the use ICG and NIR light to treat cancer in a clinical setting.

A recent report suggests that the HuH-7 human HCC cell line preferentially takes up ICG as a new mouse experimental model (74). The authors report that PDT using ICG-NIR is effective for the human HCC cell line. They evaluated three groups: ICG administration only (ICG+NIR– group), ICG administration and NIR laser exposure (ICG+NIR+ group), and NIR laser exposure without ICG administration (ICG–NIR+ group). ICG (5 mg/kg Diagnogreen; Daiichi Sankyo Co. Ltd., Tokyo, Japan) was administered intravenously via a tail vein in mice with HuH-7 cell xenografts. The HuH-7 xenograft mice were irradiated with 823 nm NIR laser 24 h after ICG administration (prototype NIR Diode Laser System, Hamamatsu Photonics, Hamamatsu, Japan). The power density was 160 mW/cm^2 for 3 min. HuH-7 tumor size was measured every 3 days. Unlike in the two control groups [ICG alone (ICG+NIR–) and neither ICG nor NIR (ICG–NIR–)], the tumor volume of the ICG+NIR+ group did not increase in the first 3 days followed by ICG-NIR PDT. Mean tumor volume did not differ significantly between the ICG–NIR+ and ICG+NIR– groups (P=0.9), but was significantly different between the ICG+NIR+ group and both the ICG–NIR+ and ICG+NIR– groups (P<0.01, both).

In their reports, developing HuH-7 tumors were observed in the center of the abdomen of the xenograft mice with no fluorescence under the fluorescence imaging system in a darkroom (*Figure 4A*). Twenty-four hours after ICG administration, the HuH-7 xenograft tumor emitted strong fluorescence under the fluorescence imaging system (*Figure 4B*). Under fluorescence microscopy, normal tissue surrounding the HuH-7 tumors produced no fluorescence, and fluorescence was observed in the cytoplasm of HuH-7 cells, but not in the nucleus (*Figure 5*).

In the same group, Shirata *et al.* focused on the mechanism of PDT and effectiveness of repeated laser irradiation (75). They found that the temperature of HuH-7 tumors increased to 48.5 ℃ in mice

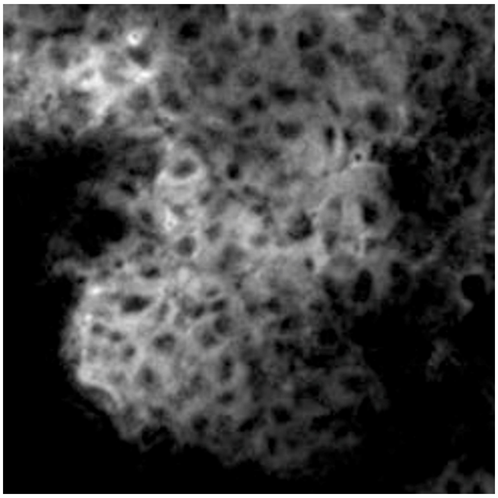

Figure 5 Under fluorescence microscopy, normal tissue surrounding HuH-7 xenograft tumors produced no fluorescence. All HuH-7 cells, however, were fluorescent. Fluorescence was observed in the cytoplasm of HuH-7 cells, but not in the nucleus.

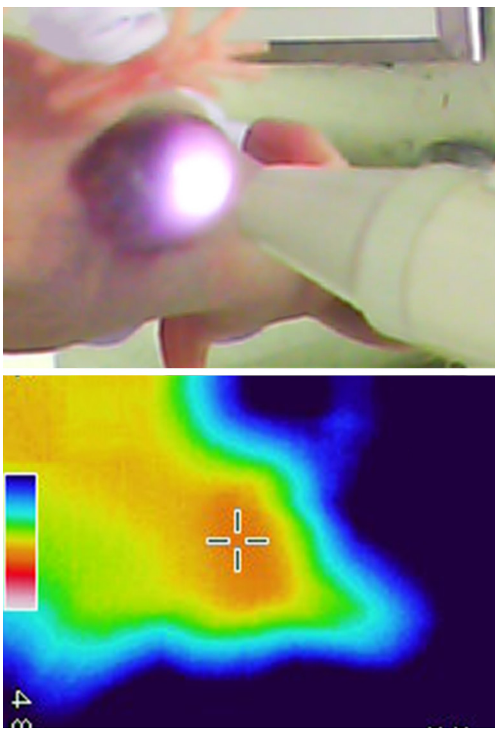

Figure 6 Temperature calibration analysis (lower panel, center of crossshaped sign) using thermography during ICG-NIR PDT. The temperature was 41.1 ℃ within 60 s after starting ICG-NIR PDT. ICG, indocyanine green; NIR, near-infrared; PDT, photodynamic therapy.

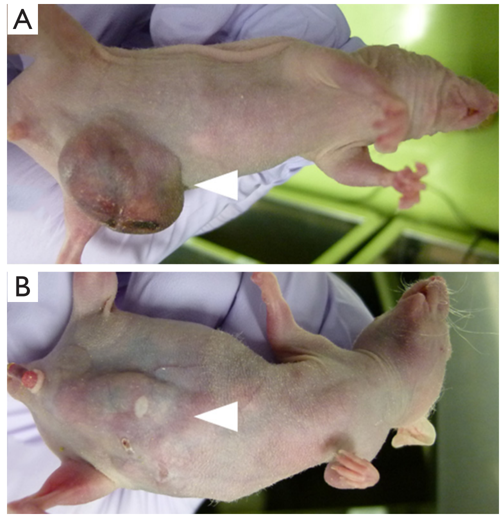

Figure 7 Large HuH-7 xenograft tumor observed in the mouse abdomen (A, triangular arrow). Later, a thin and obscure tumor was observed in the abdomen of the transplanted mice after ICG-NIR PDT (B, triangular arrow). ICG, indocyanine green; NIR, near-infrared; PDT, photodynamic therapy.

administered ICG (*Figure 6*) and 43.4 ℃ in mice without ICG. Terminal deoxynucleotidyl transferase dUTP nick end labeling analysis detected apoptosis in tumor tissues after ICG-NIR irradiation, while apoptosis was not detected in the ICG alone group. They thought that the photothermal effects contributed to the anti-tumor effect of the ICG-NIR model. Furthermore, reactive oxygen species (ROS) production was strongly detected in ICG-NIR irradiated cells compared to cells treated with ICG alone or NIR alone, or control cells *in vitro*. To analyze the production of ROS by ICG-NIR irradiation *in vivo*, they evaluated the expression of 8-hydroxy-2'-deoxyguanosine (8-OHdG) in the xenograft tumor. Positive 8-OHdG staining was detected in tumor sections after ICG-NIR irradiation, but not in tumor sections after ICG administration alone. ROS production of ICG-NIR was inhibited under the cooling condition *in vitro*. In their ICG-NIR model, the anti-tumor effect of ICG-NIR therapy against human HCC is due to apoptosis through photothermal effects and oxidative stress, and suppresses HCC cell growth by repeated NIR irradiation (*Figure 7A,B*).

In another recent experiment, Tsuda *et al.* suggested the therapeutic efficacy of ICG-loaded lactosomes for PDT for HCC in a similar mouse model (76). Lactosomes are a core-shell-type nanocarrier made of biocompatible and biodegradable material. The ICG-lactosomes accumulated in HuH-7 cell xenograft tumors and were fluorescent under NIR imaging 24 h after injection. During ICG-NIR PDT, the temperature in the xenograft tumor increased from 34.0 to 47.7 ℃ and from 34.5 to 51.7 ℃ within 0±200 s in the ICG and ICG-lactosome groups, respectively. Based on observations of tumor volume, PDT had antineoplastic effects on HuH-7 cells treated with ICG-lactosomes. Thus, several recent experiments using ICG-NIR PDT for human HCC cell line tumors in a mouse model portend a new innovative treatment for HCC, but further studies are needed to advance the clinical application.

Conclusions

In conclusion, ICG fluorescence-guided surgery may change the next generation of liver surgery. Several aspects of the mechanisms of ICG accumulation in HCC cells have been revealed by important basic research studies. In the near future, ICG-NIR PDT is expected to become a new treatment method for HCC. Although ICG is well-known and has long history in medicine, new imaging technologies and mechanistic findings keep ICG in the spotlight.

Acknowledgements

We thank Dr. Chikara Shirata and Sho Kiritani for important experiments to prove the mechanism of Indocyanine green with near-infrared light photodynamic therapy.
Funding: This work was supported by grants 17H04279 from the Ministry of Education, Culture, Sports, Science, and Technology of Japan.

Footnote

Conflicts of Interest: The authors have no conflicts of interest to declare.

References

1. Kawasaki S, Sugiyama Y, Iga T, et al. Pharmacokinetic study on the hepatic uptake of indocyanine green in cirrhotic patients. Am J Gastroenterol 1985;80:801-6.
2. Imamura H, Sano K, Sugawara Y, et al. Assessment of hepatic reserve for indication of hepatic resection: decision tree incorporating indocyanine green test. J Hepatobiliary Pancreat Surg 2005;12:16-22.
3. Clavien PA, Petrowsky H, DeOliveira ML, et al. Strategies for safer liver surgery and partial liver transplantation. N Engl J Med 2007;356:1545-59.
4. Forner A, Reig M, Bruix J. Hepatocellular carcinoma. Lancet 2018;391:1301-14.
5. Makuuchi M, Hasegawa H, Yamazaki S. Ultrasonically guided subsegmentectomy. Surg Gynecol Obstet 1985;161:346-50.
6. Shindoh J, Makuuchi M, Matsuyama Y, et al. Complete removal of the tumor-bearing portal territory decreases local tumor recurrence and improves disease-specific survival of patients with hepatocellular carcinoma. J Hepatol 2016;64:594-600.
7. Jung DH, Hwang S, Lee YJ, et al. Small Hepatocellular Carcinoma With Low Tumor Marker Expression Benefits More From Anatomical Resection Than Tumors With Aggressive Biology. Ann Surg 2017. [Epub ahead of print].
8. Miyata A, Ishizawa T, Tani K, et al. Reappraisal of a Dye-Staining Technique for Anatomic Hepatectomy by the Concomitant Use of Indocyanine Green Fluorescence Imaging. J Am Coll Surg 2015;221:e27-36.
9. Takasaki K. Glissonean pedicle transection method for hepatic resection: a new concept of liver segmentation. J Hepatobiliary Pancreat Surg 1998;5:286-91.
10. Figueroa R, Laurenzi A, Laurent A, et al. Perihilar Glissonian Approach for Anatomical Parenchymal Sparing Liver Resections: Technical Aspects: The Taping Game. Ann Surg 2018;267:537-43.
11. Ahn KS, Kang KJ, Park TJ, et al. Benefit of systematic segmentectomy of the hepatocellular carcinoma: revisiting the dye injection method for various portal vein branches. Ann Surg 2013;258:1014-21.
12. Majlesara A, Golriz M, Hafezi M, et al. Indocyanine green fluorescence imaging in hepatobiliary surgery. Photodiagnosis Photodyn Ther 2017;17:208-15.
13. Aoki T, Murakami M, Yasuda D, et al. Intraoperative fluorescent imaging using indocyanine green for liver mapping and cholangiography. J Hepatobiliary Pancreat Sci 2010;17:590-4.
14. Aoki T, Yasuda D, Shimizu Y, et al. Image-guided liver mapping using fluorescence navigation system with indocyanine green for anatomical hepatic resection. World J Surg 2008;32:1763-7.
15. Kobayashi Y, Kawaguchi Y, Kobayashi K, et al. Portal vein territory identification using indocyanine green fluorescence imaging: Technical details and short-term

outcomes. J Surg Oncol 2017;116:921-31.
16. Inoue Y, Arita J, Sakamoto T, et al. Anatomical Liver Resections Guided by 3-Dimensional Parenchymal Staining Using Fusion Indocyanine Green Fluorescence Imaging. Ann Surg 2015;262:105-11.
17. Nishino H, Hatano E, Seo S, et al. Real-time Navigation for Liver Surgery Using Projection Mapping With Indocyanine Green Fluorescence: Development of the Novel Medical Imaging Projection System. Ann Surg 2018;267:1134-40.
18. Ciria R, Cherqui D, Geller DA, et al. Comparative Short-term Benefits of Laparoscopic Liver Resection: 9000 Cases and Climbing. Ann Surg 2016;263:761-77.
19. Wakabayashi G, Cherqui D, Geller DA, et al. Recommendations for laparoscopic liver resection: a report from the second international consensus conference held in Morioka. Ann Surg 2015;261:619-29.
20. Ishizawa T, Zuker NB, Kokudo N, et al. Positive and negative staining of hepatic segments by use of fluorescent imaging techniques during laparoscopic hepatectomy. Arch Surg 2012;147:393-4.
21. Ueno M, Hayami S, Sonomura T, et al. Indocyanine green fluorescence imaging techniques and interventional radiology during laparoscopic anatomical liver resection (with video). Surg Endosc 2018;32:1051-5.
22. Kyoden Y, Tamura S, Sugawara Y, et al. Portal vein complications after adult-to-adult living donor liver transplantation. Transpl Int 2008;21:1136-44.
23. Sano K, Makuuchi M, Miki K, et al. Evaluation of hepatic venous congestion: proposed indication criteria for hepatic vein reconstruction. Ann Surg 2002;236:241-7.
24. Kubota K, Kita J, Shimoda M, et al. Intraoperative assessment of reconstructed vessels in living-donor liver transplantation, using a novel fluorescence imaging technique. J Hepatobiliary Pancreat Surg 2006;13:100-4.
25. Kawaguchi Y, Ishizawa T, Masuda K, et al. Hepatobiliary surgery guided by a novel fluorescent imaging technique for visualizing hepatic arteries, bile ducts, and liver cancers on color images. J Am Coll Surg 2011;212:e33-9.
26. Kawaguchi Y, Ishizawa T, Miyata Y, et al. Portal uptake function in veno-occlusive regions evaluated by real-time fluorescent imaging using indocyanine green. J Hepatol 2013;58:247-53.
27. Waage A, Nilsson M. Iatrogenic bile duct injury: a population-based study of 152 776 cholecystectomies in the Swedish Inpatient Registry. Arch Surg 2006;141:1207-13.
28. Rystedt JML, Tingstedt B, Montgomery F, et al. Routine intraoperative cholangiography during cholecystectomy is a cost-effective approach when analysing the cost of iatrogenic bile duct injuries. HPB (Oxford) 2017;19:881-8.
29. Jeng KS, Huang CC, Lin CK, et al. Repeated introperative cholangiography is helpful for donor safety in the procurement of right liver graft with supraportal right bile duct variants in living-donor liver transplantation. Transplant Proc 2014;46:686-8.
30. Ishizawa T, Tamura S, Masuda K, et al. Intraoperative fluorescent cholangiography using indocyanine green: a biliary road map for safe surgery. J Am Coll Surg 2009;208:e1-4.
31. Schols RM, Bouvy ND, van Dam RM, et al. Combined vascular and biliary fluorescence imaging in laparoscopic cholecystectomy. Surg Endosc 2013;27:4511-7.
32. Kaneko J, Ishizawa T, Masuda K, et al. Indocyanine green reinjection technique for use in fluorescent angiography concomitant with cholangiography during laparoscopic cholecystectomy. Surg Laparosc Endosc Percutan Tech 2012;22:341-4.
33. Mizuno S, Isaji S. Indocyanine green (ICG) fluorescence imaging-guided cholangiography for donor hepatectomy in living donor liver transplantation. Am J Transplant 2010;10:2725-6.
34. Kawaguchi Y, Velayutham V, Fuks D, et al. Usefulness of Indocyanine Green-Fluorescence Imaging for Visualization of the Bile Duct During Laparoscopic Liver Resection. J Am Coll Surg 2015;221:e113-7.
35. Diana M, Usmaan H, Legner A, et al. Novel laparoscopic narrow band imaging for real-time detection of bile leak during hepatectomy: proof of the concept in a porcine model. Surg Endosc 2016;30:3128-32.
36. Kaibori M, Ishizaki M, Matsui K, et al. Intraoperative indocyanine green fluorescent imaging for prevention of bile leakage after hepatic resection. Surgery 2011;150:91-8.
37. Gotoh K, Yamada T, Ishikawa O, et al. A novel image-guided surgery of hepatocellular carcinoma by indocyanine green fluorescence imaging navigation. J Surg Oncol 2009;100:75-9.
38. Ishizawa T, Fukushima N, Shibahara J, et al. Real-time identification of liver cancers by using indocyanine green fluorescent imaging. Cancer 2009;115:2491-504.
39. Lim C, Vibert E, Azoulay D, et al. Indocyanine green fluorescence imaging in the surgical management of liver cancers: current facts and future implications. J Visc Surg 2014;151:117-24.
40. Satou S, Ishizawa T, Masuda K, et al. Indocyanine

green fluorescent imaging for detecting extrahepatic metastasis of hepatocellular carcinoma. J Gastroenterol 2013;48:1136-43.
41. Kudo H, Ishizawa T, Tani K, et al. Visualization of subcapsular hepatic malignancy by indocyanine-green fluorescence imaging during laparoscopic hepatectomy. Surg Endosc 2014;28:2504-8.
42. Terasawa M, Ishizawa T, Mise Y, et al. Applications of fusion-fluorescence imaging using indocyanine green in laparoscopic hepatectomy. Surg Endosc 2017;31:5111-8.
43. Ishizawa T, Saiura A, Kokudo N. Clinical application of indocyanine green-fluorescence imaging during hepatectomy. Hepatobiliary Surg Nutr 2016;5:322-8.
44. Kaibori M, Matsui K, Ishizaki M, et al. Intraoperative Detection of Superficial Liver Tumors by Fluorescence Imaging Using Indocyanine Green and 5-aminolevulinic Acid. Anticancer Res 2016;36:1841-9.
45. Inoue Y, Imai Y, Fujii K, et al. The utility of 5-aminolevulinic acid-mediated photodynamic diagnosis in the detection of intraoperative bile leakage. Am J Surg 2017;213:1077-82.
46. Matsui A, Tanaka E, Choi HS, et al. Real-time intra-operative near-infrared fluorescence identification of the extrahepatic bile ducts using clinically available contrast agents. Surgery 2010;148:87-95.
47. Yoon SY, Lee CM, Song TJ, et al. A new fluorescence imaging technique for visualizing hepatobiliary structures using sodium fluorescein: result of a preclinical study in a rat model. Surg Endosc 2018;32:2076-83.
48. Zeng C, Shang W, Wang K, et al. Intraoperative Identification of Liver Cancer Microfoci Using a Targeted Near-Infrared Fluorescent Probe for Imaging-Guided Surgery. Sci Rep 2016;6:21959.
49. Andreou C, Neuschmelting V, Tschaharganeh DF, et al. Imaging of Liver Tumors Using Surface-Enhanced Raman Scattering Nanoparticles. ACS Nano 2016;10:5015-26.
50. Sekine T, Cha SH, Endou H. The multispecific organic anion transporter (OAT) family. Pflugers Arch 2000;440:337-50.
51. Konig J, Seithel A, Gradhand U, et al. Pharmacogenomics of human OATP transporters. Naunyn Schmiedebergs Arch Pharmacol 2006;372:432-43.
52. Ho RH, Tirona RG, Leake BF, et al. Drug and bile acid transporters in rosuvastatin hepatic uptake: function, expression, and pharmacogenetics. Gastroenterology 2006;130:1793-806.
53. Cui Y, Konig J, Leier I, et al. Hepatic uptake of bilirubin and its conjugates by the human organic anion transporter SLC21A6. J Biol Chem 2001;276:9626-30.
54. de Graaf W, Hausler S, Heger M, et al. Transporters involved in the hepatic uptake of (99m)Tc-mebrofenin and indocyanine green. J Hepatol 2011;54:738-45.
55. Imada S, Kobayashi T, Kitao A, et al. Central bisectionectomy for hepatocellular carcinoma in a patient with indocyanine green excretory defect associated with reduced expression of the liver transporter. Surg Case Rep 2016;2:89.
56. Kagawa T, Oka A, Kobayashi Y, et al. Recessive inheritance of population-specific intronic LINE-1 insertion causes a rotor syndrome phenotype. Hum Mutat 2015;36:327-32.
57. Kagawa T, Adachi Y, Hashimoto N, et al. Loss of organic anion transporting polypeptide 1B3 function causes marked delay in indocyanine green clearance without any clinical symptoms. Hepatology 2017;65:1065-8.
58. Ishizawa T, Masuda K, Urano Y, et al. Mechanistic background and clinical applications of indocyanine green fluorescence imaging of hepatocellular carcinoma. Ann Surg Oncol 2014;21:440-8.
59. Cherrick GR, Stein SW, Leevy CM, et al. Indocyanine green: observations on its physical properties, plasma decay, and hepatic extraction. J Clin Invest 1960;39:592-600.
60. Tazuma S, Holzbach RT. Transport of conjugated bilirubin and other organic anions in bile: relation to biliary lipid structures. Proc Natl Acad Sci U S A 1987;84:2052-6.
61. Huang L, Vore M. Multidrug resistance p-glycoprotein 2 is essential for the biliary excretion of indocyanine green. Drug Metab Dispos 2001;29:634-7.
62. Shibasaki Y, Sakaguchi T, Hiraide T, et al. Expression of indocyanine green-related transporters in hepatocellular carcinoma. J Surg Res 2015;193:567-76.
63. Jemnitz K, Heredi-Szabo K, Janossy J, et al. ABCC2/Abcc2: a multispecific transporter with dominant excretory functions. Drug Metab Rev 2010;42:402-36.
64. Verkade HJ, Wolbers MJ, Havinga R, et al. The uncoupling of biliary lipid from bile acid secretion by organic anions in the rat. Gastroenterology 1990;99:1485-92.
65. Jansen PL, van Klinken JW, van Gelder M, et al. Preserved organic anion transport in mutant TR- rats with a hepatobiliary secretion defect. Am J Physiol 1993;265:G445-52.
66. Sathirakul K, Suzuki H, Yasuda K, et al. Kinetic analysis of hepatobiliary transport of organic anions in Eisai hyperbilirubinemic mutant rats. J Pharmacol Exp Ther 1993;265:1301-12.

67. Christensen E, Mork C, Skogvoll E. High and sustained efficacy after two sessions of topical 5-aminolaevulinic acid photodynamic therapy for basal cell carcinoma: a prospective, clinical and histological 10-year follow-up study. Br J Dermatol 2012;166:1342-8.
68. Dunki-Jacobs EM, Martin RC. Endoscopic therapy for Barrett's esophagus: a review of its emerging role in optimal diagnosis and endoluminal therapy. Ann Surg Oncol 2012;19:1575-82.
69. Peng Q, Juzeniene A, Chen J, et al. Lasers in medicine. Reports on Progress in Physics 2008;71:056701.
70. Ikeda N, Usuda J, Kato H, et al. New aspects of photodynamic therapy for central type early stage lung cancer. Lasers Surg Med 2011;43:749-54.
71. Shafirstein G, Bäumler W, Hennings LJ, et al. Indocyanine green enhanced near-infrared laser treatment of murine mammary carcinoma. International Journal of Cancer 2012;130:1208-15.
72. van Gemert MC, Welch AJ. Clinical use of laser-tissue interactions. IEEE Eng Med Biol Mag 1989;8:10-3.
73. Klein A, Szeimies RM, Baumler W, et al. Indocyanine green-augmented diode laser treatment of port-wine stains: clinical and histological evidence for a new treatment option from a randomized controlled trial. Br J Dermatol 2012;167:333-42.
74. Kaneko J, Inagaki Y, Ishizawa T, et al. Photodynamic therapy for human hepatoma-cell-line tumors utilizing biliary excretion properties of indocyanine green. J Gastroenterol 2014;49:110-6.
75. Shirata C, Kaneko J, Inagaki Y, et al. Near-infrared photothermal/photodynamic therapy with indocyanine green induces apoptosis of hepatocellular carcinoma cells through oxidative stress. Sci Rep 2017;7:13958.
76. Tsuda T, Kaibori M, Hishikawa H, et al. Near-infrared fluorescence imaging and photodynamic therapy with indocyanine green lactosome has antineoplastic effects for hepatocellular carcinoma. PLoS One 2017;12:e0183527.

doi: 10.21037/tgh.2018.10.04
Cite this article as: Kaneko J, Kokudo T, Inagaki Y, Hasegawa K. Innovative treatment for hepatocellular carcinoma (HCC). Transl Gastroenterol Hepatol 2018;3:78.